Theor Chem Account (2008) 121:219–225
DOI 10.1007/s00214-008-0467-y

REGULAR ARTICLE

On the mechanism of the OH initiated oxidation of acetylene in the presence of O_2 and NO_x

Annia Galano · Luis Gerardo Ruiz-Suárez · Annik Vivier-Bunge

Received: 16 April 2008 / Accepted: 9 July 2008 / Published online: 29 July 2008

Abstract The mechanism of the oxidation of acetylene, in the presence of O_2 and NO_x, has been studied. Different levels of theory have been tested for the first step of the mechanism: the acetylene + OH radical reaction. Based on these results the meta-hybrid functional MPWB1K has been chosen for modeling all the other steps involved in the oxidation of acetylene. Different reaction paths have been considered and the one leading to glyoxal formation and OH regeneration is predicted to be the main channel, independently of the presence of NO_x. Two different mechanisms were modeled to account for formic acid formation, both of them involving cyclic intermediates. According to the computed activation free energies, the three-membered intermediate seems to be more likely to occur than the four-membered one. However, reaction barriers are very high and only a very small proportion of formic acid is expected to be formed through such intermediates. In the presence of NO_x, considered in this work for the first time, the main product of the tropospheric oxidation of acetylene is also expected to be glyoxal.

Keywords Acetylene · Oxidation · OH · NO_x · O_2 · DFT

1 Introduction

Alkynes are mainly emitted into the troposphere by biomass burning processes [1–4] and automobile emissions [5,6]. In urban areas acetylene can reach concentrations that are comparable to those of ethylene [7]. It has been calculated that the ozone impact of acetylene is approximately 2–3 times greater than that of ethane on a per-gram basis [8]. The atmospheric oxidation of acetylene is initiated by its reaction with OH radical. Several experimental studies have shown that near room temperature, the predominant mechanism of this early step involves the electrophilic addition of the OH radical to the triple bond, while there is no evidence of a hydrogen abstraction channel [9]. The acetylene contribution to tropospheric ozone production is assumed to occur via an NO to NO_2 conversion. Most of the studies on the tropospheric oxidation of acetylene have focused on the initial OH reaction, while very few have dealt with the subsequent steps, and none has considered the possible role of NO_x.

A pioneer experimental study on the atmospheric oxidation of acetylene was performed by Schmidt et al. [10]. These authors reported fast OH regeneration, most likely due to reaction of the C_2H_2–OH adduct with O_2. They also observed glyoxal as one of the oxidation products, when the process takes place in the presence of O_2. These results are in line with those by Hatakeyama et al. [11] who also reported the formation of glyoxal and formic acid when the oxidation occurs in an O_2 atmosphere and in the absence of nitrogen oxides. Accordingly, they proposed a mechanism involving O_2 addition to the C_2H_2–OH adduct, leading either to the production of glyoxal and the regeneration of OH, or evolving to a four-membered cyclic intermediate which yields formic acid and a formyl radical. The findings of Siese and Zetzsch [12] also support the OH regeneration in the presence of O_2 but in the absence of NO_x. Bohn and Zetzsch [13] proposed that HO_2 radicals are formed in the formyl radical +O_2 reaction. However, Yeung et al. [14] have not observed any hydroxy peroxy radicals in the oxidation of alkynes. These authors have also reported that a mechanism involving a

A. Galano (✉) · A. Vivier-Bunge
Departamento de Química, Universidad Autónoma Metropolitana-Iztapalapa, San Rafael Atlixco 186, Col. Vicentina, Iztapalapa, C.P. 09340 Mexico D.F., Mexico
e-mail: agalano@prodigy.net.mx

L. G. Ruiz-Suárez
Centro de Ciencias de la Atmósfera, Universidad Nacional Autónoma de México, 04510 Mexico D.F., Mexico

three-membered cyclic intermediate is thermodynamically more favored than the one proposed by Hatakeyama et al. [11]. The three-membered cyclic intermediate is similar to the one proposed by Carpenter [15] for the vinyl radical + O_2 reaction. Even though the ring is strained, its higher feasibility has been rationalized [15] in terms of the energetic cost arising from the torsional motion required for the formation of the four-membered cyclic intermediate.

Two other theoretical studies on the oxidation of acetylene have been published while this manuscript was in preparation [16,17]. In these works a different methodology, B3LYP/6-311G(3df,2p) is used and NO_x are only included semi-empirically in the master equation simulations. However, to our best knowledge, no information is available on the direct involvement of NO_x in the acetylene oxidation mechanism: the corresponding transition states structures have not been previously reported and it remains an open question to find out if the intermediates formed in the acetylene oxidation react with NO_x in a concerted or in a step-wise manner. In addition the potential formation of HNO_x, which is relevant to atmospheric chemistry, has not been analyzed.

Accordingly, it is the main aim of this work to model different reaction paths that can be potentially involved in the oxidation of acetylene, both in the presence and in the absence of NO_x, and to explicitly obtain the corresponding transition state structures, in order to be able to identify the most likely mechanism and products of the reaction.

2 Computational details

Full geometry optimizations were performed with the Gaussian 03 [18] program using the MPWB1K hybrid meta GGA functional and the 6-311++G(d,p) basis set. Unrestricted calculations were used for open shell systems. The stability of the wave functions was tested, and in all the cases they were found to be stable. Frequency calculations were carried out for all the stationary points at the same level of theory, and local minima and transition states were identified by the number of imaginary frequencies (NIMAG = 0 or 1, respectively). Intrinsic Reaction Coordinate (IRC) calculations were also performed to confirm that the transition state structures properly connect reactants and products.

The reliability of Density Functional Theory itself to properly describe chemical reaction has been discussed elsewhere (see, for example, [19–21], and references therein). In particular, the MPWB1K functional has been optimized to reproduce a large kinetics database that includes both forward and reverse barrier heights and reaction energies [22]. It has been shown that this functional yields good results for thermochemistry, thermochemical kinetics, hydrogen bonding, and weak interactions, and that it also gives excellent saddle point geometries for a variety of chemical systems [22–26].

3 Results and discussion

There is a large discrepancy among the experimentally reported values for the rate constant (k) of the acetylene + OH reaction. The values recommended by Atkinson et al. [27] and DeMore et al. [28] are almost one order of magnitude apart, at 298 K and for the high pressure limit: 9.12×10^{-12} and 8.41×10^{-13} cm^3 $molecule^{-1}$ s^{-1}, respectively. The most recent determination of k_{298} for R1 was performed by Fulle et al. [29] who obtained a value of k equal to 1.83×10^{-12} cm^3 $molecule^{-1}$ s^{-1}. These authors also reported an activation energy of 1.81 kcal/mol.

Rate coefficients for this initial step were calculated over the temperature range 200–300 K using improved canonical variational theory (ICVT) [30–33] in conjunction with small curvature tunneling (SCT) approximation, [34,35] as implemented in the POLYRATE program [36]. The potential energy surfaces were generated using multiconfigurational molecular mechanics (MCMM), [37] and the dynamic calculations on the MCMM surfaces were performed using MC-TINKERATE program [38] as interface between POLYRATE and MC-TINKER.

Within this approach, and at the high pressure limit, the rate constant of the acetylene + OH reaction has been calculated at different levels of theory (Table 1). The best agreement with the k_{298} value reported by Fulle et al. [29] was obtained at CBS-QB3 and MPWB1K/6-311++G(d,p) levels of theory, in that order, with calculated values 1.31 times higher and 1.78 times lower than the experimental value, respectively. In addition both calculated rate constants are between the two recommended values. For the calculated activation energies, on the other hand, the agreement with the experimental data was found to be better for MPWB1K/6-311++G(d,p) than for CBS-QB3. Taking into account these results, and the much higher computational cost of CBS-QB3, we have chosen MPWB1K/6-311++G(d,p) level of theory for modeling all the other steps involved in the oxidation of acetylene.

Table 1 Rate constant at 298 K (k_{298}) and Arrhenius activation energy (E_{act}) computed within the 200–300 K temperature range, for the acetylene + OH gas phase reaction

	k_{298} (cm^3 $molecule^{-1}$ s^{-1})	E_{act} (kcal/mol)
MPWB1K/6-311++G(d,p)	1.03E-12	1.28
B3LYP/6-311++G(d,p)	2.92E-10	−1.26
BH&HLYP/6-311++G(d,p)	1.16E-15	2.82
CCSD(T)//BH&HLYP/6-311++G(d,p)	2.20E-15	2.49
MP2/6-311++G(d,p)	1.01E-16	2.25
CCSD(T)//MP2/6-311++G(d,p)	2.44E-17	3.09
CBS-QB3	2.40E-12	0.95
Exp [29]	1.83E-12	1.81

Scheme 1 Modeled channels of reaction for the OH initiated oxidation of acetylene

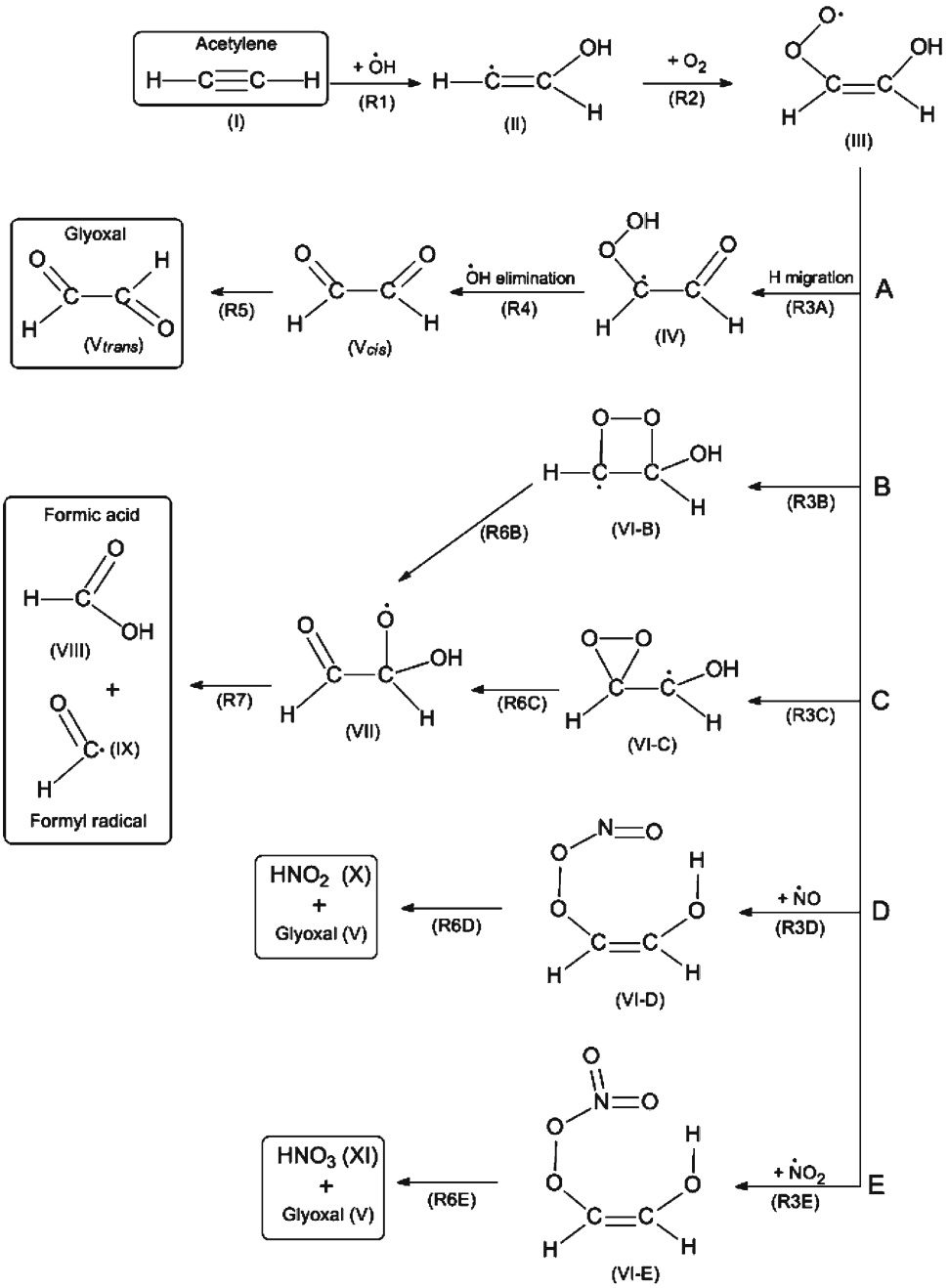

It seems relevant to emphasize the fact that the results recently reported by Maranzana et al. [16,17] were obtained at B3LYP/6-311G(3df,2p) level of theory. However, according to the results in Table 1, this widely used functional (B3LYP) significantly disagree with the experimental data, at least for the initial step of the acetylene oxidation. Theory-experiment comparisons for validating the used methodology have been performed only for this step since there are no other experimental data reported.

It is well accepted that the determining step in the oxidation of most unsaturated volatile organic compounds is the initial addition of the hydroxyl radical (R1, in Scheme 1). The main geometrical parameters of the transition state corresponding to this initial step (TS-1, Fig. 1) are: distance r(C···O) = 2.031 Å, angle a(OCC) = 108.8, and dihedral angle d(OOCC) = 0. This addition process is exothermic and exergonic, and occurs through a reaction barrier of 7.45 kcal/mol, with respect to isolated reactants and in terms of Gibbs free energy (Table 2).

After the OH adduct (II) is formed, and in the presence of O_2, reaction R2 yields a hydroxyperoxyl radical (III) in which the OH fragment is bonded to one carbon atom and

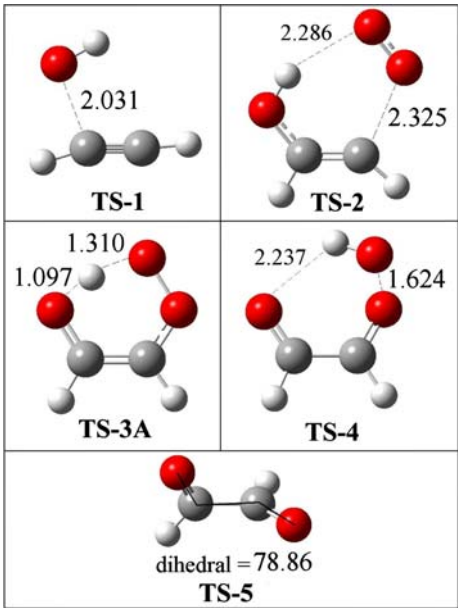

Fig. 1 Optimized geometries of the transition states involved in glyoxal formation. All molecular graphics have been constructed using GaussView visualization program [39]

the OO fragment is bonded to the other carbon. The geometry of the transition state for the reaction of intermediate II with O_2 (R2 in Scheme 1) is shown in Fig. 1. This process is also exothermic and exergonic, with a free energy activation of 10 kcal/mol. The alternative formation of *trans*-III was also computed and it was found that, compared to the formation of the *cis* conformer, this process is less exergonic by 5.6 kcal/mol and that its barrier is higher by 2.23 kcal/mol. This means that most of structure III is expected to occur in its *cis* form (97.7%). Accordingly, in this work the acronym III refers to the *cis* conformer.

Once radical III is formed there are several potentially viable reaction paths that can compete and yield different products. It has been reported that the main product of reaction is glyoxal, and that OH regeneration is observed [10–12]. In addition, formic acid has also been reported to be formed in the absence of NO_x. In this work five possible reaction paths have been studied (A to E in Scheme 1), in order to determine which ones are most likely to lead to the observed products. Channels A, B and C do not require the presence of NO_x, while D and E could represent tropospheric pathways. Two of the mechanisms (B and C) have been proposed earlier [11,14] in order account for the formation of formic acid. They involve cyclic intermediates: a four membered [11] and a three-membered [14] ring.

Path A leads to glyoxal formation and OH regeneration. It includes: (i) a hydrogen migration from the hydroxyl group to the peroxyl end (R3A), followed by (ii) OH elimination (regeneration) and the formation of *cis*-glyoxal (R4), which eventually evolves to the most stable conformer: *trans*-glyoxal (R5).

According to our results the H migration has an activation free energy of only 0.32 kcal/mol (Table 2). The formed product (IV) is lower in energy than III, both in terms of enthalpy and Gibbs free energy, so that this process is expected to be very fast. The OH elimination requires overcoming a barrier of 8.12 kcal/mol and is exothermic and exergonic. Once the *cis*-glyoxal (V*cis*) is formed, its conversion to the *trans* form involves a very low barrier (1.59 kcal/mol). Therefore the whole path A is expected to occur in almost a cascade way.

Path B, which was first proposed by Hatakeyama et al., [11] involves the cyclization (R3B) of structure III to form a four-membered cyclic intermediate (VI-B), the opening of the cyclic structure to yield VII (R6B), and the C–C rupture of VII to produce formic acid (VIII) and formyl radical (IX). The structures of the transition states corresponding to the cyclic intermediate formation (TS-3B) and to the opening of the ring (TS-6B) are shown in Fig. 2. Reaction R3B does not seem to be a viable process. It needs to overcome a very high barrier (∼37 kcal/mol) and, moreover, it is endothermic and endergonic in 17.06 and 17.46 kcal/mol, respectively. It can be argued that structure III is formed with a large excess of energy, which could be used in the formation of VI-B, however this excess is smaller than the barrier (∼35 kcal/mol). Accordingly even if we assume that no collisions have occurred after the formation of III and that it is able to conserve all the energy excess, it still would not be sufficient to overcome the barrier involved in the formation

Table 2 Classical barriers ($\Delta E^{\neq}$) and heats of reaction (ΔE), enthalpies of reaction (ΔH), Gibbs free energies of reaction (ΔG) and barriers ($\Delta G^{\neq}$) at 298.15 kcal/mol

Reaction[a]	ΔE[b]	ΔH	ΔG	$\Delta E^{\neq}$ [b]	$\Delta G^{\neq}$
R1	−38.18	−35.06	−26.69	0.26	7.45
R2	−50.20	−46.95	−35.16	0.88	10.04
R3A	−4.76	−5.24	−5.52	2.89	0.32
R3B	17.12	17.06	17.46	38.51	37.43
R3C	10.70	10.09	9.38	23.36	21.87
R3D	−17.45	−15.80	−4.41	3.68	14.47
R3E	−18.79	−16.04	−2.80	1.65	14.16
R4	−11.53	−14.76	−25.94	10.64	8.12
R5	−4.77	−4.68	−3.90	1.40	1.59
R6B	−68.15	−69.00	−70.54	10.16	8.25
R6C	−61.74	−62.03	−62.46	14.59	13.71
R6D	−47.78	−49.86	−63.26	1.01	0.61
R6E	−45.17	−47.22	−60.31	3.29	2.20
R7	−8.22	−10.32	−21.49	2.42	1.53

[a] Refers to 1
[b] Calculated from electronic energies

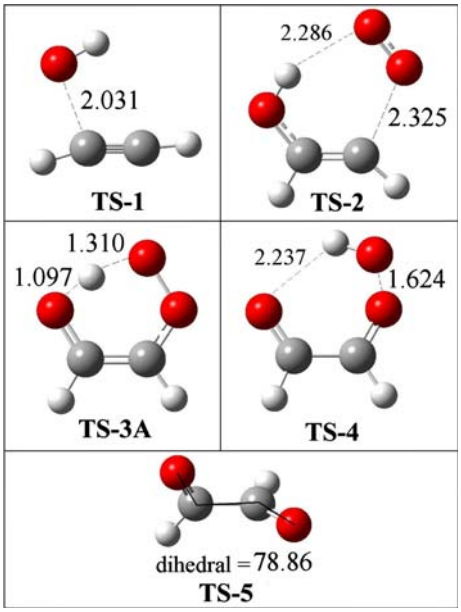

Fig. 2 Optimized geometries of the transition states involved in cyclic products formation

of the four-membered cyclic intermediate. In addition, the formation of this cyclic intermediate would have to compete with the fast H-migration (3A) reaction. Thus, the present calculations seem to rule out this mechanism as an explanation for formic acid formation.

The mechanism proposed by Yeung et al. [14] to explain the formic acid formation has also been modeled (Path C). It involves a three-membered cyclic intermediate (VI-C) formed from structure III (R3C) and the opening of VI-C to yield VII (R6C), which in turn would produce formic acid (VIII) and formyl radical (IX) through the C–C bond cleavage of compound VII. In this case the barrier involved in the cyclic intermediate is also high, albeit much lower than the one needed to form the four -membered cycle (VI-B). The free energy of activation associated with R3C is found to be equal to 21.87 kcal/mol. This value is lower than the excess energy of III (∼35 kcal/mol) and, in principle, the process could be feasible. However reaction R3C is endergonic by 9.38 kcal/mol. Also, as in the case of R3B, the formation of the cyclic intermediate would have to compete with the fast H-migration (3A) reaction.

Assuming that VI-C is formed before structure III is thermalyzed, the three-membered intermediate can then evolve either through the opening of the O–O bond, yielding radical VII (R6C), or through the C–O bond cleavage leading back to structure III (–R3C). R6C involves the migration of the H atom in the OH group to one of the oxygens in the cycle, and its activation free energy is found to be equal to 13.71 kcal/mol, while $\Delta G^{\neq}$(-R3C) = 12.69 kcal/mol. Since these barriers differ by only 1 kcal/mol, and the formation

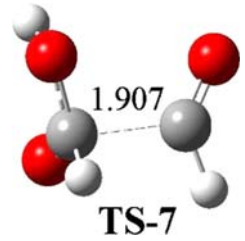

Fig. 3 Optimized geometry of the C–C rupture transition state involved in formic acid formation

of VII is a very exergonic process (−62.46 kcal/mol), i.e. highly irreversible, it seems reasonable to assume that structure VII could be formed to a significant extent. The structure of the transition state involved in the next step, which corresponds to the C–C rupture of VII, is shown in Fig. 3. This process (R7) involves a very low barrier (1.53 kcal/mol) and it is expected to occur very rapidly. In addition, R7 is exothermic and exergonic by 10.32 and 21.49 kcal/mol, respectively. Thus, according to our results, and considering that formic acid is a minor product of acetylene oxidation, path C seems to be a viable mechanism. However, since the formation of VI-C would be prevented by the collisional stabilization of radical III, path C would necessarily be highly pressure dependent.

Up to this point, none of the studied paths have included the potential role of NO_x on the atmospheric oxidation of acetylene. On the other hand, Paths D and E, proposed in this work for the first time, take them into account. In our opinion it is important to consider NO_x radicals in this study

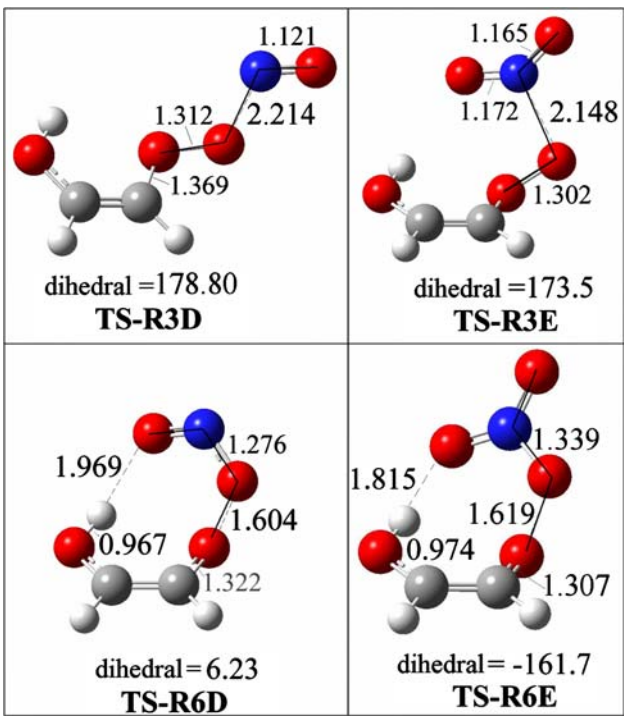

Fig. 4 Optimized geometries of the transition states for paths involving NO_x

because they are abundant tropospheric compounds that are directly involved in ozone production.

Path D involves the NO radical addition to the peroxyl end of III (R3D), followed by HNO_2 elimination (R6D) and glyoxal formation. The conversion of the peroxyl radical to an oxyl radical by NO was also considered. Actually the transition state structure TS-R6D (Fig. 4) was found as the possible TS of such conversion. However when the corresponding IRC calculation was performed it was clear that the connecting products were glyoxal + HNO_2, instead of oxyl radical + NO_2. Any further attempt to find a different TS structure invariably leads to the same TS geometry, i.e. the NO_2 elimination occurs concertedly with the hydrogen abstraction. In addition the energy release for reaction R6D was found to be larger than that of the oxyl formation by 46.0, 46.1 and 46.8 kcal/mol in terms of Gibbs free energy, enthalpy, and electronic energy; respectively. Then, and based on the Hammond postulate, it seems reasonable to assume that even if the hypothetical oxyl TS exists it should be higher in energy than TS-T6D.

An alternative path (E) involving NO_x would occur by addition of an NO_2 radical to the peroxyl end of III (R3E), followed by HNO_3 elimination (R6E) and glyoxal formation. The free energies of activation associated with the additions of NO and NO_2 to structure III were found to be very similar, with values of $\Delta G^{\neq}$(R3D) and $\Delta G^{\neq}$(R3E) equal to 14.47 and 14.16 kcal/mol, respectively. In addition the exothermicity and exergonicity of both processes are also similar (Table 2). After the corresponding adducts are formed the HNO_2 or HNO_3 eliminations (R6D or R6E) are expected to occur very fast since both processes involve very low barriers: $\Delta G^{\neq}$(R6D) = 0.61 kcal/mol and $\Delta G^{\neq}$(R6E) = 2.2 kcal/mol. In addition, reactions R6D and R6E are significantly exergonic with $\Delta G^{\neq}$(R6D) and $\Delta G^{\neq}$(R6E) equal to −63.26 and −60.31 kcal/mol, respectively. Accordingly, paths D and E are both feasible in the presence of NO_x and they also contribute to the formation of glyoxal. In addition nitrous and nitric acids are formed.

The free energy profiles of all the modeled reaction paths are shown in Fig. 5. Comparing the barriers associated with the possible evolution of structure III it becomes evident that the process that is most likely to occur corresponds to path A, i.e. leading to glyoxal formation and OH regeneration. This mechanism is predicted to be the main reaction path in the presence of O_2, and independently of the presence of NO_x. Thus, path A would be the main reaction channel, both in laboratory chambers free of NO_x and in the troposphere. In NO_x-free environments and at high pressure limit, only a very minor amount of formic acid is predicted to be formed, since the associated barriers are quite high. In this case, the process would proceed through the formation of a three-membered cyclic intermediate. Paths D and E are energetically more favored than B and C and no formic acid

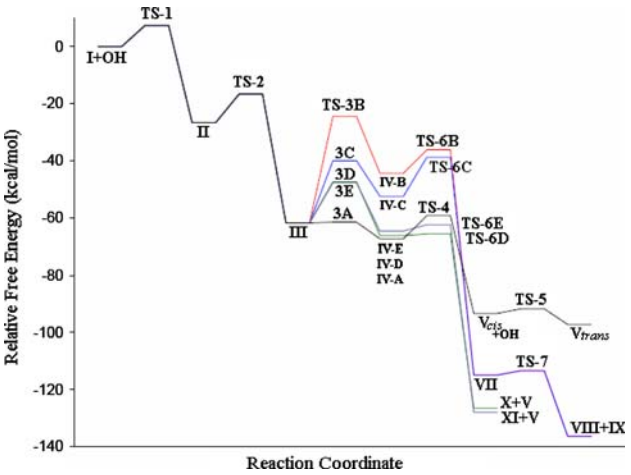

Fig. 5 Gibbs free energy evolution involved in the atmospheric oxidation of acetylene

is expected to be formed through such channels. Since there is a significant presence of NO_x in the troposphere, particularly in urban areas, HNO_2 and HNO_3 are expected to be formed to an extent that would depend on the concentrations of NO and NO_2, respectively. This finding might be relevant to tropospheric chemistry since these contaminants play a significant role in acid rain.

However, the molecularities of the competing R3 paths are not the same: R3A, R3B and R3C are unimolecular processes while R3D and R3E are bimolecular. Accordingly, in addition to the analysis of the Gibbs free energy evolution, the corresponding rate constant have been estimated taking into accounts concentrations of NO and NO_2 of 0.5 ppm, which correspond to moderately polluted atmospheres [40]. Under these conditions, the estimated values at 298 K are 3.6×10^{12}, 2.3×10^{-15}, 5.8×10^{-4}, 7.7×10^{-5} and $1.3\times10^{-4}\,s^{-1}$ for R3A, R3B, R3C, R3D and R3E, respectively. Therefore glyoxal is expected to be the only significant product formed from the reaction channels considered in 1. It is clear that pathways B and C cannot explain the 40% formic acid formation reported by Hatakeyama et al. [11]. The latter might be explained by photochemical processes instead, however they are outside the aim of the present work.

4 Conclusions

The oxidation of acetylene in the presence of O_2 and NO_x has been studied at MPWB1K/6-311++G(d,p) level of theory. Different reaction paths have been computed, and the one leading to glyoxal formation and OH regeneration (Path A) is predicted to be the main reaction channel, independently of the presence of NO_x.

Two different mechanisms were modeled in an effort to explain the observed formation of formic acid in the absence

of NO_x. According to the computed free energies of activation, only the path involving a three-membered ring might occur, although it would have to be at very low pressures and only very small quantities of formic acid would be formed through that channel.

In the presence of NO_x, considered in this work for the first time, the alternative pathways (R3D and R3E) are energetically much more favored than those leading to formic acid formation (R3B and R3C). However, taking into account the tropospheric concentrations of NO and NO_2 the corresponding rate constant would also be very low, compared to that of path R3A. Accordingly, glyoxal is expected to be the only significant product formed from the reaction channels in 1.

Acknowledgments The authors thank the SEPCONACYT grant SEP-2004-C01-46167 for the financial support and Prof. J. R. Alvarez-Idaboy for his useful comments. A.G. also thanks professors D. G. Truhlar, O. Tishchenko and J. Zheng for their valuable help and advice regarding the use of programs POLYRATE and MC-TINKERATE.

References

1. Greenberg JP, Zimmerman PR, Heidt L, Pollock W (1984) J Geophys Res 89:1350. doi:10.1029/JD089iD01p01350
2. Greenberg JP, Zimmerman PR (1984) J Geophys Res 89:4767. doi:10.1029/JD089iD03p04767
3. Hegg DA, Radke LF, Hobbs PV, Rasmussen RA, Riggan PJ (1990) J Geophys Res 95:5669. doi:10.1029/JD095iD05p05669
4. Blake NJ, Blake DR, Sive BC, Rowland FS, Collins JE Jr, Sachse GW, et al (1996) J Geophys Res 101:24151. doi:10.1029/96JD00561
5. Stephens ER, Burleson FR (1967) J Air Pollut Control Assoc 17:147
6. Fraser MP, Cass GR, Simoneit BR (1998) Environ Sci Technol 32:2051. doi:10.1021/es970916e
7. Calvert JG, Atkinson R, Kerr JA, Madronich S, Moortgat GK, Wallington TJ et al (2000) The Mechanisms of Atmospheric Oxidation of the Alkenes. Oxford University Press, New York
8. Carter WPL (1994) J Air Waste Manage Assoc 44:881
9. Sorenson M, Kaiser EW, Hurley D, Wallington TJ, Nielsen O (2003) Int J Chem Kinet 35:191. doi:10.1002/kin.10119
10. Schmidt V, Zhu GY, Becker KH, Fink EH (1985) Ber Bunsenges Phys Chem 89:321
11. Hatakeyama S, Washida N, Akimoto H (1986) J Phys Chem 90:173. doi:10.1021/j100273a039
12. Siese M, Zetzsch C (1995) Z Phys Chem 188:75
13. Bohn B, Zetzsch C (1998) J Chem Soc, Faraday Trans 94:1203. doi:10.1039/a708536b
14. Yeung LY, Pennino MJ, Miller AM, Elrod MJ (2005) J Phys Chem A 109:1879. doi:10.1021/jp0454671
15. Carpenter BK (1995) J Phys Chem 99:9801. doi:10.1021/j100024a022
16. Maranzana A, Barker JR, Tonachini G (2008) J Phys Chem A, ASAP Article. doi:10.1021/jp077180k
17. Maranzana A, Ghigo G, Tonachini G, Barker JR (2008) J Phys Chem A, ASAP Article. doi:10.1021/jp077174o
18. Gaussian 03, Revision C.02, Frisch MJ, Trucks GW, Schlegel HB, Scuseria GE, Robb MA, Cheeseman JR, Montgomery JA Jr, Vreven T, Kudin KN, Burant JC, Millam JM, Iyengar SS, Tomasi J, Barone V, Mennucci B, Cossi M, Scalmani G, Rega N, Petersson GA, Nakatsuji H, Hada M, Ehara M, Toyota K, Fukuda R, Hasegawa J, Ishida M, Nakajima T, Honda Y, Kitao O, Nakai H, Klene M, Li X, Knox JE, Hratchian HP, Cross JB, Adamo C, Jaramillo J, Gomperts R, Stratmann RE, Yazyev O, Austin AJ, Cammi R, Pomelli C, Ochterski JW, Ayala PY, Morokuma K, Voth GA, Salvador P, Dannenberg JJ, Zakrzewski VG, Dapprich S, Daniels AD, Strain MC, Farkas O, Malick DK, Rabuck AD, Raghavachari K, Foresman JB, Ortiz JV, Cui Q, Baboul AG, Clifford S, Cioslowski J, Stefanov BB, Liu G, Liashenko A, Piskorz P, Komaromi I, Martin RL, Fox DJ, Keith T, Al-Laham MA, Peng CY, Nanayakkara A, Challacombe M, Gill PMW, Johnson B, Chen W, Wong MW, Gonzalez C, Pople JA (2004) Gaussian Inc., Wallingford
19. Siegbahn PEM, Blomberg MRA (1999) Ann Rev Phys Chem 50:221
20. Ziegler T (1991) Chem Rev 91:651
21. Fernandez-Ramos A, Miller JA, Klippenstein SJ, Truhlar DG (2006) Chem Rev 106:4518. doi:10.1021/cr050205w
22. Zhao Y, Truhlar DG (2004) J Phys Chem A 108:6908
23. Zhao Y, Schultz NE, Truhlar DG (2006) J Chem Theory Comput 2:364
24. Zhao Y, Truhlar DG (2005) J Phys Chem A 109:5656
25. Zhao Y, Truhlar DG (2005) J Chem Theory Comput 1:415
26. Zhao Y, Gonzalez-Garcia N, Truhlar DG (2005) J Phys Chem A 109:2012
27. Atkinson R, Baulch DL, Cox RA, Hampson RF, Kerr JA, Rossi MJ, Troe J (1997) J Phys Chem Ref Data 26:521
28. DeMore WB, Sander SP, Golden DM, Hampson RF, Kurylo MJ, Howard CJ, Ravishankara AR, Kolb CE, Molina MJ (1997) JPL Publication 97:1
29. Full D, Hamann HF, Hippler H, Jansch CP (1997) Ber Bunsenges Phys Chem 101:1433
30. Garrett BC, Truhlar DG, Grev RS, Magnuson AW (1980) J Phys Chem 84:1730
31. Garrett BC, Truhlar DG, Grev RS, Magnuson AW (1983) J Phys Chem 87:4554(E)
32. Issacson AD, Truhlar DG (1982) J Chem Phys 76:1380
33. Isaacson AD, Sund MT, Rai SN, Truhlar DG (1985) J Chem Phys 82:1338
34. Skodje RT, Truhlar DG, Garrett BC (1981) J Phys Chem 85:3019
35. Liu YP, Lynch GC, Truong TN, Lu D, Truhlar DG (1993) J Am Chem Soc 115:2408
36. Corchado JC, Chuang YY, Fast PL, Villa J, Hu WP, Liu YP, Lynch GC, Nguyen KA, Jackels CF, Melissas VS, Lynch BJ, Rossi I, Coitino EL, Fernandez-Ramos A, Ellingson BA, Pu J, Albu TV, Zheng J, Steckler R, Garrett BC, Isaacson AD, Truhlar, DG (2007) POLYRATE, Version 9.7, University of Minnesota, Minneapolis
37. Kim Y, Corchado JC, Villa J, Xing X, Truhlar DG (2000) J Chem Phys 112:2718
38. Albu TV, Tishchenko O, Corchado JC, Kim Y, Villa J, Xing J, Lin H, Truhlar DG (2007) MC-TINKERATE; Version P9.1, University of Minnesota, Minneapolis
39. Dennington R, Keith T, Millam J, Eppinnett K, Hovell WL, Gilliland R (2003) GaussView, Version 2.0, Semichem Inc., Shawnee Mission
40. Finlayson-Pitts BJ, Pitts JN (1986) Atmospheric chemistry: fundamentals and experimental techniques. Wiley, New York